

See discussions, stats, and author profiles for this publication at: <https://www.researchgate.net/publication/231525292>

# Multichromophoric Cyclodextrins. 4. Light Conversion by Antenna Effect

ARTICLE in JOURNAL OF THE AMERICAN CHEMICAL SOCIETY · JUNE 1996

Impact Factor: 12.11 · DOI: 10.1021/ja954332t

---

CITATIONS

88

---

READS

30

8 AUTHORS, INCLUDING:



Ludovic Jullien

Ecole Normale Supérieure de Paris

139 PUBLICATIONS 3,043 CITATIONS

SEE PROFILE

Valérie Marchi-Artzner

French National centre for scientific research...

47 PUBLICATIONS 1,551 CITATIONS

SEE PROFILE



Robert Bernard Pansu

French National Centre for Scientific Research

130 PUBLICATIONS 2,041 CITATIONS

SEE PROFILE

## Multichromophoric Cyclodextrins. 4. Light Conversion by Antenna Effect

Ludovic Jullien,<sup>\*,†,||</sup> Josette Canceill,<sup>†</sup> Bernard Valeur,<sup>\*,‡,§</sup> Elisabeth Bardez,<sup>‡,§</sup> Jean-Pierre Lefèvre,<sup>‡,§</sup> Jean-Marie Lehn,<sup>\*,†</sup> Valérie Marchi-Artzner,<sup>†</sup> and Robert Pansu<sup>§</sup>

*Contribution from the Collège de France, Laboratoire de Chimie des Interactions Moléculaires (CNRS UPR 285), 11 Place Marcelin Berthelot, 75005 Paris, Conservatoire National des Arts et Métiers, Laboratoire de Chimie Générale, 292 rue Saint-Martin, 75003 Paris, Ecole Normale Supérieure de Cachan, Laboratoire de Photophysique et Photochimie Supramoléculaires et Macromoléculaires (CNRS URA 1906), 61 Avenue du Président Wilson, 94235 Cachan Cedex, and Ecole Normale Supérieure (Ulm), Département de Chimie (CNRS URA 1679), 24 rue Lhomond, 75005 Paris, France*

Received December 29, 1995<sup>®</sup>

**Abstract:** A water soluble  $\beta$ -cyclodextrin (CD-NA) bearing seven naphthoyl chromophores forms very stable 1:1 complexes with a merocyanine laser dye DCM-OH (4-(dicyanomethylene)-2-methyl-6-(*p*-(bis(hydroxyethyl)amino)-styryl)-4*H*-pyran). The antenna effect, i.e. energy transfer from the naphthoyl antenna chromophores to the encased dye, is shown to occur with 100% efficiency. The stability of the complexes is very high ( $K_s \approx 10^5$ ) owing to the contribution of the naphthoate residues. The structural features of the complexes have been examined in detail: circular dichroism experiments confirm the expected axial orientation of DCM-OH in the cavity of CD-NA, and fluorescence anisotropy measurements together with  $^{13}\text{C}$ -NMR longitudinal relaxation time measurements show that the complex formed between CD-NA and DCM-OH is tight. The mechanisms of homotransfer (i.e., between naphthoate chromophores) and heterotransfer (i.e., from naphthoate chromophores to DCM-OH included in the cavity) are discussed in light of existing theories. In both cases, the major contribution arises more likely from Coulombic interaction than from short-range interactions. Such multichromophoric cyclodextrins are good models for mimicry of the antenna function in photosynthesis and show great promise as photochemical microreactors.

### Introduction

The primary processes of photosynthesis are light absorption, energy migration, and transfer to the reaction center of the photosynthetic units.<sup>1,2</sup> These processes occur in chloroplast pigments whose photon-harvesting efficiency is very high owing to the large number of chlorophyll–protein complexes they contain; excitation energy migrates among chlorophyll molecules within the pigment and is eventually trapped in the reaction center where it is converted into chemical energy. Such an enhancement of light sensitivity due to an increase of the overall cross section for light absorption is called the “antenna effect”. The antenna pigments act also as a protective valve in the case of excess of radiation.

The antenna effect has already been studied in artificial systems such as polymers having chromophores substituted at intervals along the chains,<sup>3,4</sup> complexes between lanthanide ions and polypyridine ligands,<sup>5</sup> polynuclear complexes,<sup>6,7</sup> and multichromophoric cyclodextrins.<sup>8</sup> The interest in these studies is not only to provide a better understanding of the light-harvesting

step of photosynthesis but also to design photomolecular devices for conversion of light (solar energy conversion, frequency conversion of light, luminescent labels of biological interest, etc.).<sup>9</sup>

In the previous papers of this series,<sup>10–12</sup> we described the synthesis of  $\beta$ -cyclodextrins labeled with seven or 14 chromophores, and the photophysical studies showed that energy hopping among chromophores is fast, not chaotic but directed toward lower-energy chromophores. The dynamics of energy hopping among chromophores was also studied theoretically and by time-resolved experiments. We reported also recently preliminary results on the efficient antenna effect occurring in a new multichromophoric  $\beta$ -cyclodextrin CD-NA, i.e. energy transfer from seven antenna chromophores to a merocyanine inserted in the cavity.<sup>8</sup> The present paper aims at fully

(6) Balzani, V. In *Photoprocesses in Transition Metal Complexes, Biosystems and Other Molecules. Experiment and Theory*; Kochanski, E., Ed.; Kluwer Academic Publishers: Dordrecht, The Netherlands, 1992; p 233.

(7) Scandola, F.; Bignozzi, C. A.; Chiorboli, C.; Indelli, M. T.; Rampi, M. A. In *Photoprocesses in Transition Metal Complexes, Biosystems and Other Molecules. Experiment and Theory*; Kochanski, E., Ed.; Kluwer Academic Publishers: Dordrecht, The Netherlands, 1992; p 253.

(8) Jullien, L.; Canceill, J.; Valeur, B.; Bardez, E.; Lehn, J.-M. *Angew. Chem., Int. Ed. Engl.* **1994**, *33*, 2438.

(9) Balzani, V.; Scandola, F. *Supramolecular Photochemistry*; Horwood: New York, 1990.

(10) Berberan-Santos, M. N.; Canceill, J.; Brochon, J. C.; Jullien, L.; Lehn, J. M.; Pouget, J.; Tauc, P.; Valeur, B. *J. Am. Chem. Soc.* **1992**, *114*, 6427.

(11) Berberan-Santos, M. N.; Pouget, J.; Valeur, B.; Canceill, J.; Jullien, L.; Lehn, J.-M. *J. Phys. Chem.* **1993**, *97*, 11376.

(12) Berberan-Santos, M. N.; Canceill, J.; Gratton, G.; Jullien, L.; Lehn, J.-M.; Peter So, P.; Sutin, J.; Valeur, B. *J. Phys. Chem.* **1996**, *100*, 15.

<sup>†</sup> Collège de France.

<sup>‡</sup> Conservatoire National des Arts et Métiers.

<sup>§</sup> Ecole Normale Supérieure (Cachan).

<sup>||</sup> Ecole Normale Supérieure (Ulm).

<sup>®</sup> Abstract published in *Advance ACS Abstracts*, May 1, 1996.

(1) *Antennas and Reaction Centers in Photosynthetic Bacteria*; Michel-Beyerle, M. E., Ed.; Springer Verlag: New York, 1985.

(2) *The Photosynthetic Bacterial Reaction Center—Structure and Dynamics*; Breton, J.; Vermeglio, H., Eds.; Plenum Press: New York, 1988.

(3) Guillet, J. E. *Polymer Photophysics and Photochemistry*; Cambridge University Press: Cambridge, U.K., 1985.

(4) Webber, S. E. *Chem. Rev.* **1990**, *90*, 1469.

(5) (a) Alpha, B.; Lehn, J.-M.; Mathis, G. *Angew. Chem.* **1987**, *99*, 1310; *Angew. Chem., Int. Ed. Engl.* **1987**, *26*, 266. (b) Sabbatini, N.; Guardigli, M.; Lehn, J.-M. *Coord. Chem. Rev.* **1993**, *123*, 201.

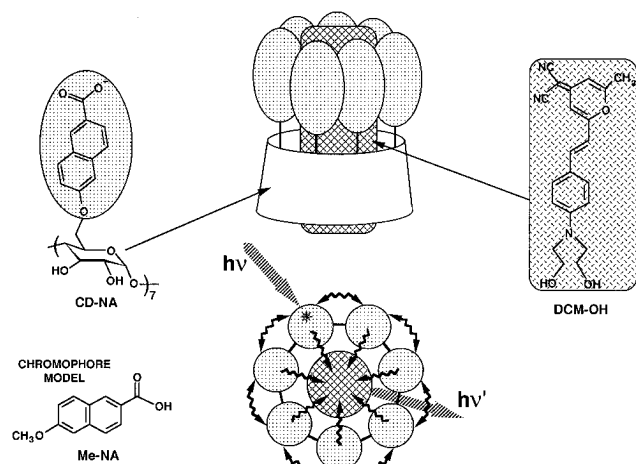
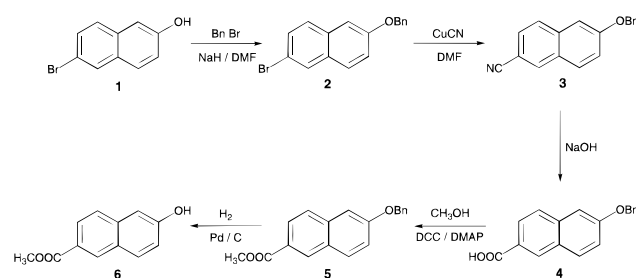
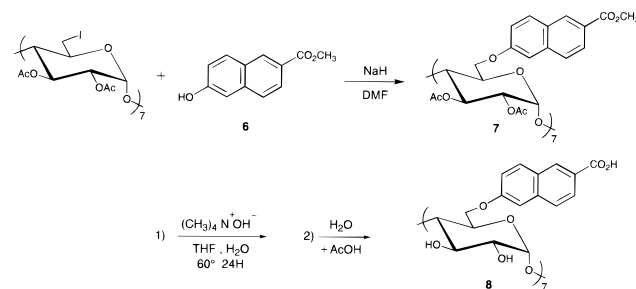


**Figure 1.** Schematic illustration of the complex between the heptanaphthoate  $\beta$ -cyclodextrin CD-NA and the merocyanine DCM-OH.

### Scheme 1



### Scheme 2



describing light conversion by antenna effects in such complexes (Figure 1) via a thorough characterization of the complexes.

### Synthesis

CD-NA was obtained from condensation of the naphthoate chromophore on a  $\beta$ -cyclodextrin derivative. The naphthoate part was synthesized in five steps from 2-bromo-6-hydroxy naphthalene (**1**) (Scheme 1): (i) benzylation of the alcohol position to give **2** (BnBr, NaH, DMF; heat ( $\Delta$ )); (ii) cyanation from bromine atom exchange to yield **3** (CuCN, DMF;  $\Delta$ ); (iii) hydrolysis of the cyano group to give **4** (NaOH,  $\Delta$ ); (iv) esterification of the acid to provide **5** (MeOH, DCC, DMAP); (v) hydrogenolysis to finally afford **6** ( $\text{H}_2$ , Pd/C 10%,  $\text{CH}_2\text{Cl}_2$ , MeOH; room temperature (RT)). Ethyl 2-hydroxy-6-naphthoate ester (**6**) was then condensed on the per-2,3-di-acetyl, per-6-iodo- $\beta$ -cyclodextrin<sup>13</sup> to yield the perester **7** (NaH, DMF; RT), which was eventually hydrolyzed to give CD-NA **8** (TMAOH, THF,  $\text{H}_2\text{O}$ ;  $\Delta$ ; then  $\text{H}_2\text{O}$ , AcOH) (Scheme 2).

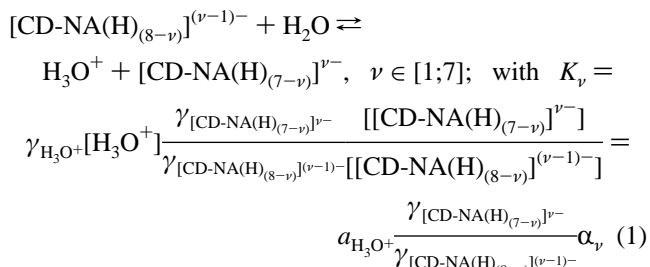
(13) Baer, H. H.; Shen, Y.; Gonzalez, F. S.; Berenguel, A. V.; Garcia, J. I. *Carbohydr. Res.* **1992**, 235, 129. Guillo, F.; Hamelin, B.; Jullien, L.; Canceill, J.; Lehn, J.-M.; De Robertis, L.; Driguez, H. *Bull. Soc. Chim. Fr.* **1995**, 132, 857.

### Photophysical Properties of the Multichromophoric Cyclodextrin CD-NA

**Absorption Spectra.** In contrast to the multichromophoric cyclodextrins described in our previous work,<sup>10–12</sup> CD-NA is soluble in water at pH higher than about 6. When increasing pH above this value, the absorption spectrum undergoes an hypsochromic shift because of ionization of the naphthoate chromophores (from  $\lambda_{\text{max}} = 296$  nm at pH 6 to  $\lambda_{\text{max}} = 288$  nm at pH > 6); no further evolution is observed at pH values beyond 8. This behavior is to be compared with that of the model chromophore Me-NA (2-methoxy-6-naphthoic acid) whose  $\text{pK}_a$  value, as checked by UV spectra, is 4.3 and which exhibits a similar spectral shift up to pH = 6, without further evolution beyond 6. The  $\text{pK}_a$  values for CD-NA seem then to be increased with regard to Me-NA.

At pH = 10 where CD-NA may be considered as fully deprotonated, and at ionic strength  $\mu = 0.1$  M, the absorbance follows the Beer–Lambert law in the range of concentrations that was used in this study, thus strongly suggesting that CD-NA is present as a monomer in solution. Moreover, it should be noted that, beyond pH 8, the normalized absorption spectra of Me-NA and CD-NA are almost identical, which means that there is no significant interaction in the ground state between the naphthoate groups of CD-NA.

The acidobasic properties of CD-NA deserve further comment, especially the shift of its apparent last  $\text{pK}_a$  with respect to that of Me-NA and the absence of a strong influence of ionic strength on this  $\Delta\text{pK}_a$  shift (*vide infra*). These properties can be rationalized under consideration of acidobasic equilibria taking place for CD-NA:



where the  $\gamma_i$  are the activity coefficients and the  $[i]$  the concentrations of the species  $i$ . The first term  $a_{\text{H}_3\text{O}^+}$ , the proton activity, is measured from the pH of the solution. The second term measures the deviation from ideality (reference state: infinitely diluted solution of CD-NA in water). Since the electrostatic interactions are expected to play the major role for deviation from ideality and since the Debye–Hückel reciprocal length  $\kappa^{-1}$  at ionic strengths used throughout this study is much less than the average CD-NA–CD-NA distance,<sup>14</sup>  $\gamma_{[\text{CD-NA(H)}_{(7-v)}]^{v-}} \approx \gamma_{[\text{CD-NA(H)}_{(8-v)}]^{(v-1)-}} \approx 1$  constitutes a good approximation. The last term,  $\alpha_v$ , is evaluated from UV spectra.

In a first approximation, the intrinsic standard Gibbs free energy ( $\Delta_R G^\circ$ ) associated with the proton dissociation in the 6-alkoxy-2-naphthoic acid function in aqueous solutions can be reasonably assumed to be constant.  $K_v$  and  $\Delta_R G^\circ$  can be linked together according to the relation<sup>15</sup>

(14)  $\kappa^{-1}$  remains inferior to 5 nm under all conditions of this study and is inferior to 1 nm at  $\mu = 0.1$  M whereas  $\langle R \rangle$  lies in the 8 nm range.

(15) Hamelin, B.; Jullien, L.; Guillo, F.; Lehn, J.-M.; Jardy, A.; DeRobertis, L.; Driguez, H. *J. Phys. Chem.* **1995**, 99, 17877.

$$pK_v = -\log_{10}\left(\frac{8-\nu}{\nu}\right) + \log_{10}\left(\frac{\Delta_R G^\circ}{RT}\right) + \frac{e^2}{4\pi \ln 10 k T \epsilon_0 \epsilon_r R_{CD}}(\nu - 1) = \text{pH} - \log_{10} \alpha_\nu \quad (2)$$

where  $e$  is the elementary proton charge,  $k$  the Boltzmann constant,  $\epsilon_0$  the dielectric constant of vacuum,  $\epsilon_r$  the relative dielectric constant of the medium, and  $R_{CD}$  the radius of the assumed circular crown of acidic groups. As  $\log_{10}(\Delta_R G^\circ/RT)$  can be equalized to the  $pK$  of Me-NA, eq 2 shows that the last CD-NA  $pK_7$  ( $\alpha_7 = 1$ ) is shifted toward higher values compared to  $pK(\text{Me-NA})$  by about 2.7 units when taking  $\epsilon_r = 78.3$  at 298 K and  $R_{CD} = 1$  nm.<sup>16</sup> This crude estimate is in reasonable agreement with the experimental observation of this study and of others;<sup>17</sup> the  $pK$  of the model was estimated to be equal to 4.3, whereas the highest  $pK_a$  of CD-NA may be about 7, as shown by the lack of any noticeable change above  $\text{pH} = 8$ .

**Emission Spectra.** In order to avoid any change in the emission spectra due to displacements of prototropic equilibria in the ground state, the fluorescence emission is considered at  $\text{pH}$  values greater than 8; then the spectrum remains unchanged (at constant ionic strength) and consists of two bands located at 355 and 405 nm, in contrast to the model chromophore which does not exhibit a band at 405 nm (Figure 2). In order to check whether this band is due to ground-state species or not, excitation spectra were recorded upon observation at 355 and 405 nm: they were both found to be almost identical to the absorption spectrum (the slight differences arising from some imperfection of the correction procedure). Therefore, the band at 405 nm results from an excited-state process which can be either protonation of the naphthoate groups (leading to the emission of the resulting naphthoic form which is expected around 400 nm) or excimer formation. However, excited-state protonation is a diffusion-controlled process and is unlikely to occur during the excited-state lifetime in a basic medium where  $\text{pH} > 8$ , i.e.  $[\text{H}_3\text{O}^+] < 10^{-8}$  M, whatever the excited-state  $pK_a^*$  values of the carboxylic groups. Therefore, excimer formation is the likely explanation, as supported by time-resolved experiments (vide infra). It should be noted that excimers were identified in  $\beta$ -CD labeled with naphthoxy chromophores<sup>10</sup> and in those labeled with naphthalene-6-sulfonate residues.<sup>17</sup> In contrast, the band at 405 nm is absent in the fluorescence spectrum in ethanol of the precursor of CD-NA **7**, i.e. with methyl ester groups instead of carboxylic groups. The absence of excimer formation is surprising at first sight; it may be explained in terms of steric hindrance and better solvation of the aromatic chromophores in organic solvents.

**Ionic Strength Effects on Absorption and Emission Spectra.** Figure 3A,B displays the ratio of absorbances of CD-NA at 296 and 288 nm and the ratio of fluorescence intensities at 350 nm and 420 nm at two ionic strengths ( $5 \times 10^{-3}$  and 0.1 M) as a function of  $\text{pH}$ . In both cases, these ratios vary similarly and level off at  $\text{pH} 7$ . This result is consistent with the following phenomena whose relative contributions are difficult to assess: (i) a contribution in the absorption and emission spectra of some 2-alkoxy-6-naphthoic acid chromophores that are present at  $\text{pH}$  below 7 (vide supra) (the acid form of Me-NA exhibits a maximum of emission at 406 nm); (ii) a larger contribution of excimer formation either intra- or intermolecular. The decrease of the number of charges borne at chromophore extremities is expected to reduce the average naphthoyl–naphthoyl distance and to decrease the activation energy to form excimers, thus promoting intramolecular excimer formation. Furthermore,

(16) Under assumption that the dielectric constant of the solvent is not modified by salt addition which is a good approximation until  $\mu = 0.1$  M.

(17) Gravett, D. M.; J. Guillet, *J. Am. Chem. Soc.* **1993**, *115*, 5970.

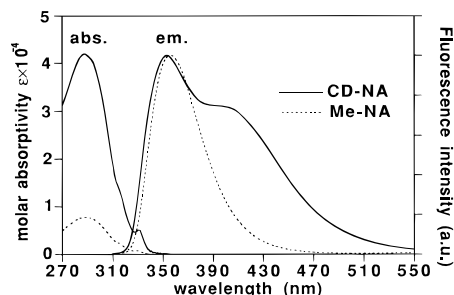


**Figure 2.** Absorption and corrected fluorescence spectra of CD-NA and the model compound Me-NA in a buffer at  $\text{pH} 10$ . For comparison, the fluorescence spectra have been normalized to the same height at the maximum.

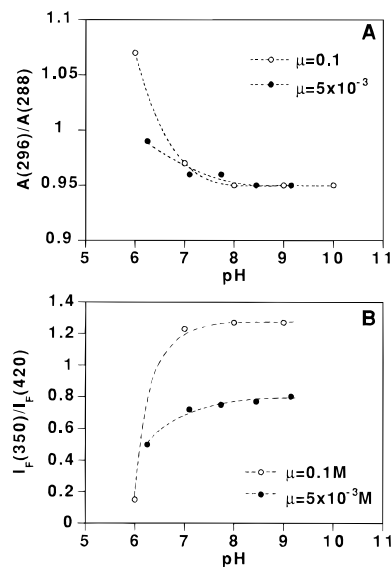


**Figure 3.** Effect of  $\text{pH}$  on the ratio of absorbances (A) and fluorescence intensities (B) at two wavelengths for CD-NA.

since CD-NA is not water-soluble in acidic media, it is possible that small aggregates begin to form as soon as CD-NA is not anymore fully deprotonated, i.e. below  $\text{pH} = 7$ –8.

Ionic strength is expected to change the apparent value of  $pK_7$  in two ways: (i) nonspecifically by modifying the concentration of protons close to the highly negatively charged  $[\text{CD-NA}]^{7-}$  at a given  $\text{pH}$ . The local decrease in proton concentration when increasing the concentration of supporting electrolyte, i.e.  $\mu$ , should thus be accompanied with an apparent decrease of  $pK_7$  provided that local application of acidobasic equilibria concepts are valid; (ii) specifically by shifting possible equilibria involving the complexation of the cation from the supporting electrolyte by the negatively charged CD-NA crown of carboxylate groups. The latter effect should lead to an apparent increase of  $pK_7$  when increasing  $\mu$ . The present experiments suggest that, in the range that has been investigated, ionic strength does not play a major role for significant shift of  $pK_a$ .

Ionic strength exerts a strong influence on fluorescence spectra. Figure 4 shows the evolution of intensity ratio at 355 and 410 nm of fluorescence emission of CD-NA at  $\text{pH} = 10$  and at different ionic strengths while keeping the same buffer constituents. The obtained curve displays a maximum around  $\mu = 0.1$  M, the ratio being smaller below and above this value. The monotonously decreasing branch of the curve can be accounted on the basis of dependence of the Debye–Hückel length  $\kappa^{-1}$  on ionic strength. Above  $\mu = 0.1$  M,  $\kappa^{-1}$  becomes inferior to the estimated averaged distance between carboxylic groups (1 nm). This means that, above this ionic strength,

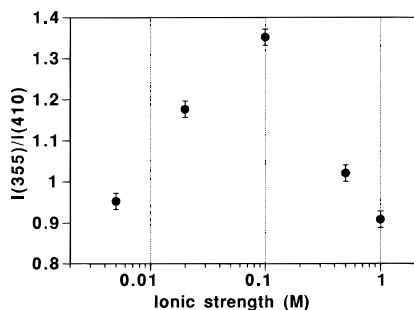


**Figure 4.** Effect of ionic strength on the ratio of fluorescence intensities at two wavelengths for CD-NA in a buffer at pH 10.

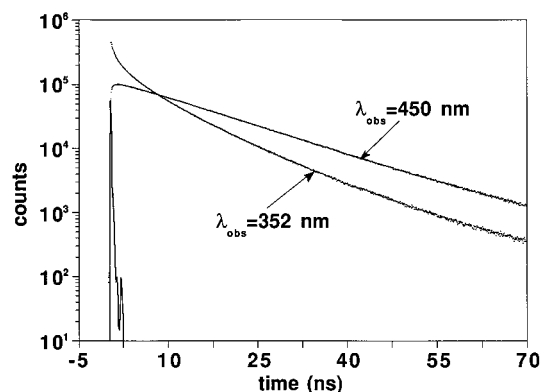


**Figure 5.** Fluorescence decay curves of CD-NA in a buffer at pH 10 containing 5% (v/v) of ethanol (excitation at 290 nm; observation at 352 and 450 nm). The instrument response function is represented as a line.

electrostatic repulsion between chromophores becomes efficiently screened and that excimer formation becomes more favorable as  $\mu$  increases. The other part of the curve is much more difficult to explain. We can tentatively suppose that a conformational change occurs at low ionic strengths. Under these conditions where the electrostatic repulsion between identically charged groups is maximum, it is possible that the average of chromophore configurations of lowest energy does not belong to the  $C_7$  symmetry. In this case, configurations involving more asymmetrically distributed and possibly head to tail organized naphthoyl groups should be involved; the head to tail organization is suitable to promote excimer formation while keeping the negative charges away to decrease electrostatic repulsion.

The above results on pH and ionic-strength dependence led us to perform all subsequent photophysical experiments at pH 10 and  $\mu = 0.1$  M, i.e. under conditions where all chromophores are in the naphthoate form and where excimer formation is minimum since excimers act as traps in the energy migration process.

**Fluorescence Decays.** The fluorescence decay curves of CD-NA (2.9  $\mu$ M) at pH 10 were recorded at 352 and 450 nm upon excitation by a picosecond laser pulse at 290 nm (Figure 5); the time resolution of the instrument is 45 ps. At 352 nm, where emission from the monomer form of the naphthoate groups is predominant, the fluorescence decay is very complex. Analysis of the data using a nonlinear least-squares method shows that a sum of four exponentials is not sufficient to get a satisfactory fit. A very fast initial decay is to be noticed. At 450 nm, where emission from the excimer form is predominant, the response is also complex and it is difficult to get reliable values of the parameters; nevertheless, there is a very fast initial rise of the fluorescence (with two or more risetimes) followed by a decay. The existence of a fast initial decay at 352 nm and a fast initial

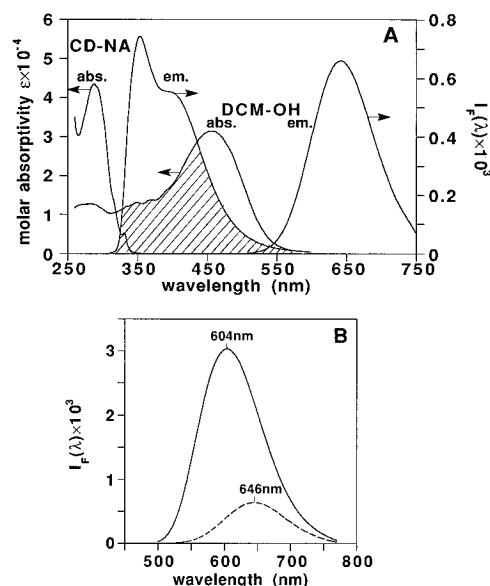


**Figure 6.** (A) Absorption spectra and corrected fluorescence spectra of CD-NA and DCM-OH in a buffer at pH 10 containing 5% (v/v) of ethanol. The region where the fluorescence spectrum of CD-NA overlaps the absorption spectrum of DCM-OH is cross-hatched. (B) Corrected fluorescence spectra of DCM-OH (3.5  $\mu$ M) in the absence (broken line) and in the presence of CD-NA (62  $\mu$ M) (solid line). In both parts A and B of this figure, the fluorescence spectra are normalized to the quantum yield ( $\Phi_F = \int_0^\infty I_F(\lambda) d\lambda$ ).

rise at 450 nm in addition to the fact that the longer decay time is found to be about 14.3 ns are compelling evidence for excimer formation from naphthoate monomers, as anticipated from steady-state spectra. The complexity of the data is certainly due to the formation of different types of excimers. It is beyond the scope of the present paper to attempt further analysis of the time-resolved data by other methods, e.g. the maximum entropy method.

In our previous work<sup>10</sup> devoted to multichromophoric cyclodextrins with appended naphthoyloxy groups, no rise time was detected in the shortest time scale available with our instrumentation, which was interpreted in terms of small displacement required for excimer formation. The fact that the naphthoyloxy groups are neutral, while the naphthoate residues of the present CD-NA are charged, may explain a longer time required for excimer formation in the latter case.

### Energy Transfer to an Acceptor in the Cavity. Antenna Effect

**Choice of the Acceptor.** The main criteria that the acceptor should fulfill in order to observe an efficient energy transfer from the antenna chromophores are (i) the formation of stable complexes with CD-NA, (ii) a good overlap of the acceptor absorption spectrum with the emission spectrum of CD-NA, (iii) a low absorbance of the acceptor at wavelengths around the absorption maximum of CD-NA.

A good candidate is DCM-OH (4-(dicyanomethylene)-2-methyl-6-(*p*-(bis(hydroxyethyl)amino)styryl)-4*H*-pyran),<sup>18</sup> a derivative of the well-known laser dye DCM (4-(dicyanomethylene)-2-methyl-6-(*p*-(dimethylamino)styryl)-4*H*-pyran). The spectral characteristics of DCM-OH are shown in Figure 6A, where the good spectral overlap of its absorption spectrum with the emission spectrum of CD-NA is clearly seen.

In addition to these favorable spectral characteristics, efficient complexation of DCM-OH with CD-NA is expected because

(18) Bourson, J.; Doizi, D.; Lambert, D.; Sacaze, T.; Valeur, B. *Opt. Commun.* **1989**, 72, 367.

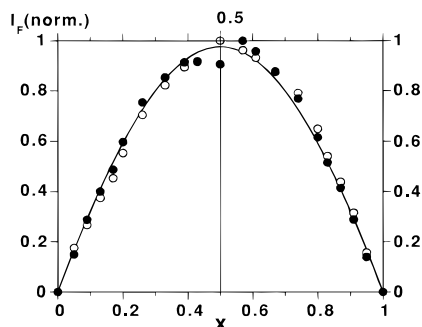


**Figure 7.** Job's plot: variations of  $(I_F - xI_1)$  at 590 nm as a function of  $x = [\text{DCM-OH}]/([\text{DCM-OH}] + [\text{CDNA}])$ , at constant sum of concentrations ( $[\text{DCM-OH}] + [\text{CDNA}] = 2.9 \mu\text{M}$ ).  $I_1$  is the fluorescence intensity for  $x = 1$ , i.e. without CD-NA. Solvent: buffer at pH 10 containing 5% (v/v) of ethanol. Excitation wavelength: 300 nm (open circles); 400 nm (closed circles).

its elongated form is consistent in size with the CD-NA interior, as its length is approximately equal to the depth of the cavity plus the length of the linked chromophores; moreover, it is essentially hydrophobic but partially hydrophilic thanks to the two terminal hydroxylic groups (DCM-OH is fairly soluble in water containing a small amount of ethanol).

#### Evidence for Complexation of CD-NA with DCM-OH.

The fluorescence quantum yield of DCM-OH in a buffer at pH 10 containing 5% (v/v) of ethanol increases by a factor of about 5 on addition of CD-NA up to a 19-fold excess, and its fluorescence spectrum undergoes a blue shift of ca. 40 nm (Figure 6B). For the interpretation of this blue shift, it is worth recalling that the dipole moment of DCM—and consequently DCM-OH—is much higher in the excited state than in the ground state;<sup>19</sup> therefore, the higher the polarity of the solvent, the larger the red shift of the fluorescence spectrum as a result of solvent relaxation. A blue shift of the fluorescence spectrum of DCM-OH is thus consistent with a more hydrophobic environment experienced by DCM-OH in the CD's cavity and with a reduction of solvent relaxation.

Job's plot<sup>20</sup> yields a simple way to determine the stoichiometry of the complex. The fluorescence intensity  $I_F$  of DCM-OH is monitored at 590 nm as a function of the fraction  $x = [\text{DCM-OH}]/([\text{DCM-OH}] + [\text{CD-NA}])$ , at constant sum of concentrations ( $[\text{DCM-OH}] + [\text{CD-NA}]$ ). The variation of  $(I_F - xI_1)$ , where  $I_1$  is the fluorescence intensity for  $x = 1$  (i.e., in the absence of CD-NA), is plotted versus  $x$  (Figure 7). The curve passes through a maximum at 0.5 which means that DCM-OH forms a 1:1 complex with CD-NA. Strictly speaking, analysis according to Job's method only proves that the stoichiometry is  $n:n$ , but circular dichroism spectra show that only one molecule of DCM-OH is included in the CD cavity (*vide infra*), so that the stoichiometry is in fact 1:1.

Further characterization of the complex (stability constant, structural features, etc.) will be presented below.

**Antenna Effect.** Solutions ( $2.9 \mu\text{M}$ ) of CD-NA in the pH 10 buffer containing 5% (v/v) of ethanol and various amounts of DCM-OH were prepared. The fluorescence of the naphthoate residues (excited at 300 nm) decreases as the concentration of DCM-OH increases (Figure 8). This quenching process arises from energy transfer from the naphthoate residues to DCM-

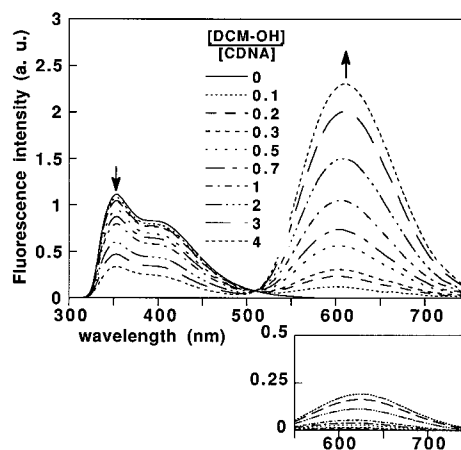


**Figure 8.** Evolution of the fluorescence spectrum of a CD-NA solution on addition of DCM-OH from a concentration ratio  $[\text{DCM-OH}]/[\text{CD-NA}] = 0-4$  (solvent: buffer at pH 10 containing 5% (v/v) of ethanol). Excitation wavelength: 300 nm. Bottom: contribution from DCM-OH molecules directly excited at 300 nm (see text).

OH, as confirmed by the concomitant increase in fluorescence intensity of the latter. Attention is to be paid to the contribution of the directly excited DCM-OH molecules (at 300 nm) to this increase; this contribution was obtained by measuring the fluorescence spectra upon excitation at 400 nm, where there is no absorption of CD-NA, and by multiplying them by the ratio of the absorbances at 300 and 400 nm. Correction was made for the difference in lamp intensities at these wavelengths. This contribution turned out to be only a small fraction of the overall DCM-OH fluorescence. The main reason is that the quantum yield of DCM-OH in the buffer is much lower than in the CD's cavity (see Figure 6B).

Information on the rate and efficiency of transfer is in principle provided by time-resolved fluorescence experiments upon excitation of the donor and observation of either the donor or the acceptor. The fluorescence decay of the naphthoate residues excited at 290 nm and observed at 352 nm was recorded in the absence and in the presence of 4-fold excess of DCM-OH (Figure 9). The decays were found to be superimposable (after normalization at the same height at the maximum in order to compensate for the large decrease in fluorescence intensity in the presence of DCM-OH; see Figure 8). This important result means that the observed fluorescence in the 320–500 nm region is solely due to CD-NA's containing no DCM-OH molecule and that the fluorescence of the naphthoate groups belonging to complexes is totally quenched; *the efficiency of transfer from the naphthoate chromophores to DCM-OH is thus very close to 1*. Note also that the ratio of fluorescence intensity at 410 and 355 nm remains constant upon addition of DCM-OH, which means that the efficiencies of transfer from naphthoate monomers and excimers (if they still exist in the complex) are both close to 1.

As a consequence of such a high transfer efficiency, no information on the rate of transfer can be drawn from the decay of the naphthoate residues. This prompted us to observe the time-resolved emission of DCM-OH upon excitation at 300 nm with the hope to see a rise of the fluorescence intensity due to transfer from the naphthoate groups. No rise time was detected with our instrumentation (resolution of 45 ps), which means that the transfer rate is shorter than a few tens of picoseconds.

Before discussing the mechanism of energy transfer, a thorough characterization of the complex of CD-NA with DCM-OH is desirable.

(19) (a) Meyer, M.; Mialocq, J. C.; Perly, B. *J. Phys. Chem.* **1990**, *94*, 98. (b) Marguet, S.; Mialocq, J. C.; Millié, Ph.; Berthier, G.; F. Momicchioli, F. *Chem. Phys.* **1992**, *160*, 265.

(20) Connors, K. A. *Binding Constants. The Measurement of Complex Stability*; Wiley: New York, 1987.

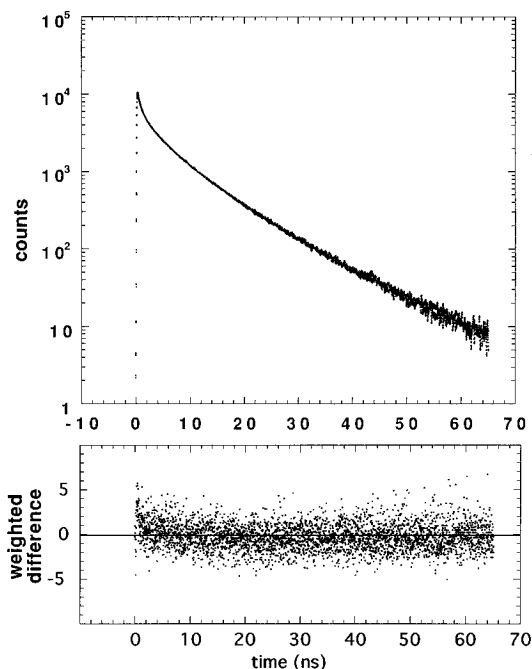
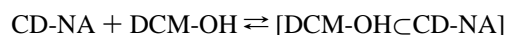


**Figure 9.** Fluorescence decays of CD-NA (2.9  $\mu\text{M}$ ) excited at 290 nm and observed at 352 nm in the absence and in the presence of DCM-OH (4-fold excess). The decays have been normalized at the same height at the maximum for comparison. Bottom: weighted difference between the two decays after normalization. Solvent: buffer at pH 10 containing 5% (v/v) of ethanol.

### Characterization of the complex of CD-NA with DCM-OH

**Stability of the Complex  $[\text{DCM-OH} \subset \text{CD-NA}]$ .** The stability constant for the equilibrium



can be determined in different ways. The most straightforward way is to monitor the decrease in fluorescence intensity of the naphthoate residues (upon excitation at 300 nm) as DCM-OH is added at constant CD-NA concentration. Figure 10A shows the variations at 355, 394, and 430 nm which are identical. These variations have been corrected for inner-filter effects because the amount of light absorbed by DCM-OH in the region where the naphthoate residues emit becomes more and more significant as DCM-OH is added. The correction factors were determined by monitoring the fluorescence intensity of the model compound Me-NA upon addition of DCM-OH under the same conditions, i.e. in the same solvent mixture and at a concentration such that the absorbance at 300 nm is exactly the same as that of the CD-NA solution.

The corrected data are then analyzed on the basis that the stoichiometry of the complex is 1:1 (*vide supra*), for which the following formula can be easily obtained (see, for instance, ref 21)

$$I_F = I_0 - \frac{I_0 - I_{\text{lim}}}{2} \times \left\{ \left( 1 + R + \frac{1}{c_0 K_s} \right) - \left[ \left( 1 + R + \frac{1}{c_0 K_s} \right)^2 - 4R \right]^{1/2} \right\} \quad (3)$$

where  $I_0$  is the initial fluorescence intensity,  $I_{\text{lim}}$  is the intensity at full complexation,  $c_0$  is the total concentration in CD-NA,  $R$  is the ratio  $[\text{DCM-OH}]_{\text{tot}}/[\text{CD-NA}]_{\text{tot}}$  (i.e., the number of equivalents), and  $K_s$  is the stability constant of the 1:1 complex.

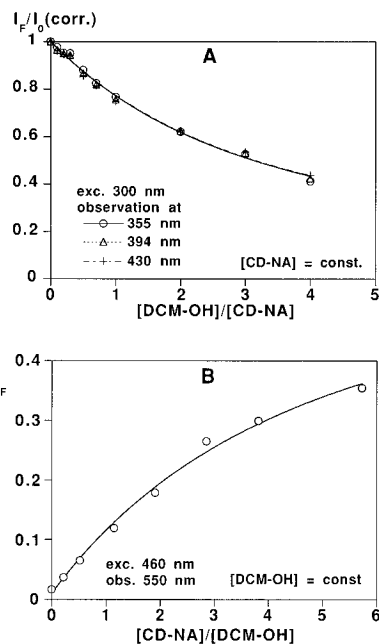


**Figure 10.** (A) Variations in fluorescence intensity of CD-NA (excitation at 300 nm) upon addition of DCM-OH at constant CD-NA concentration (2.9  $\mu\text{M}$ ). The variations have been corrected for inner-filter effects. The solid line is the best fit with eq 1: the stability constant of the complex is  $(1.2 \pm 0.2) \times 10^5$  (correlation coefficient: 0.998). (B) Variations in fluorescence intensity of DCM-OH (excitation at 460 nm) upon addition of CD-NA at constant DCM-OH concentration (2.27  $\mu\text{M}$ ). The solid line is the best fit with eq 1: the stability constant of the complex is  $(1.0 \pm 0.3) \times 10^5$  (correlation coefficient: 0.997). Solvent: buffer at pH 10 containing 5% (v/v) of ethanol.

$I_{\text{lim}}$  is taken to be zero since the transfer efficiency is 1 and, therefore, there is no fluorescence emission from the naphthoate at full complexation. The only unknown parameter is then  $K_s$ , and curve fitting with a nonlinear least-squares method yields a value of  $(1.2 \pm 0.2) \times 10^5$ . If  $I_{\text{lim}}$  is taken as a floating parameter, a value close to zero is recovered.

Another way to determine the stability constant is to monitor the fluorescence intensity of DCM-OH (upon excitation at 460 nm where CD-NA does not absorb) as CD-NA is added at constant DCM-OH concentration. The variation in fluorescence intensity observed at 550 nm due to environmental changes upon insertion in the cavity is plotted in Figure 10B. Equation 1 can still be used but with  $R$  representing now the ratio  $([\text{CD-NA}]_{\text{tot}}/[\text{DCM-OH}]_{\text{tot}})$  and  $c_0$  is the total concentration of DCM-OH. Curve fitting yields  $K_s = (1.0 \pm 0.3) \times 10^5$ , which is in good agreement with the method using naphthoate fluorescence.

### Structural Features of the Complex with DCM-OH.

Circular dichroism experiments are expected to provide information on orientation of DCM-OH with respect to the axis of CD-NA. Figure 11 shows induced circular dichroism (ICD) spectra of a solution of CD-NA in the absence and in the presence of DCM-OH (4-fold excess). A positive band is observed in the absorption region of DCM-OH. The absence of any Cotton effect proves that only one DCM-OH molecule is included in the CD-NA cavity, which is evidence for 1:1 stoichiometry of the complex. Furthermore, the correlation between structure and chiroptical properties of cyclodextrin complexes with aromatic molecules has been expressed by Kajtar and co-workers<sup>22</sup> in the form of a simple rule by which the relative arrangement of guest and host can be estimated from the ICD spectrum. In the present case, the transition dipole

(21) Bourson, J.; Pouget, J.; Valeur, B. *J. Phys. Chem.* **1993**, 97, 4552.

(22) Kajtar, M.; Horváth-Toró, Cs.; Kuthi, E.; Szejtli, J. *Acta Chim. Acad. Sci. Hung.* **1982**, 110, 327.

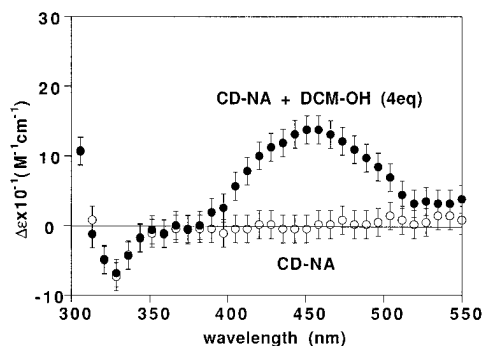


**Figure 11.** Circular dichroism spectra of a solution of CD-NA (2.9  $\mu\text{M}$ ) without and with DCM-OH (4-fold excess). Solvent: buffer at pH 10 containing 5% (v/v) of ethanol.

moment of DCM-OH is oriented along the long axis and the positive ICD band means that this transition dipole moment falls within an imaginary double cone whose center coincides with that of cyclodextrin and whose generating line forms an angle of about  $30^\circ$  with the  $C_7$  symmetry axis. This confirms the expected axial orientation of DCM-OH in the cavity of CD-NA.

It is now of interest to elucidate whether the complex is tight or loose. This characteristic can be deduced from fluorescence polarization experiments; emission anisotropy of DCM-OH is in fact related to the rotational correlation time. As the transition dipole moment of DCM-OH is oriented along the long axis, rotation around this axis has insignificant effect on emission anisotropy and only rotation around the short axis is effective. Therefore, roughly speaking, rotational motions of DCM-OH can be considered as isotropic.

The data on steady-state emission anisotropy  $\bar{r}$  and lifetime  $\tau$  of DCM-OH are reported in Table 1. The fluorescence decay in the presence of cyclodextrin is double exponential with a short decay time corresponding to the lifetime of free DCM-OH and a longer one corresponding to the lifetime in the CD-NA cavity; the former is indeed close to the lifetime measured in the absence of CD-NA. The fact that the lifetime is much shorter in the buffer than in the cavity is consistent with the findings on fluorescence quantum yields: the ratio of lifetimes is 5.2, i.e. identical to the ratio of quantum yields. The value of 0.390 measured for the emission anisotropy in glycerol at  $-5^\circ\text{C}$ , i.e. in a solvent that is viscous enough to preclude significant rotation during the lifetime of the excited state, represents the fundamental anisotropy  $r_0$ . Then, using Perrin's relation for isotropic rotations, rewritten as

$$\frac{1}{\bar{r}} = \frac{1}{r_0} \left( 1 + \frac{\tau}{\tau_c} \right) \quad (4)$$

the rotational correlation time  $\tau_c$  of DCM-OH in the pH 10 buffer is found to be 0.30 ns.

At first sight, it seems surprising that the emission anisotropy is slightly smaller in the presence of cyclodextrin even though rotational motions are hindered in the complex. This is due to the fact that the lifetime of DCM-OH is much shorter (0.5 ns) in the buffer than in the cavity (2.5 ns). With an excess of CD-NA by a factor of 18.8, the contribution of free DCM-OH to the overall intensity is very small, and a good estimate of the correlation time can thus be drawn from eq 4. The found value is  $\tau_c = 1.3$  ns, i.e. more than four times larger than that of free DCM-OH. Under the same conditions, a time-resolved anisotropy experiment shows that the anisotropy decay is a single exponential with a correlation time of 1.4 ns.

In order to see whether the complex formed between CD-NA and DCM-OH is tight or loose, this value of the DCM-OH

correlation time is now to be compared with the correlation time of CD-NA. Unfortunately, the latter cannot be determined from fluorescence anisotropy measurements because energy transfer between naphthoyl chromophores is a most efficient way to promote fluorescence depolarization (in addition to the possible fast local motions of the chromophores). *A priori*, the CD-NA correlation time should be obtained from  $^{13}\text{C}$ -NMR longitudinal relaxation time  $T_1$  measurements. Nevertheless, the required high concentration of CD-NA to perform the NMR experiment, just as the complexity to prepare the deuterated buffer solution, led us to perform the  $T_1$  determination on the perester precursor **7** in  $\text{CD}_2\text{Cl}_2$  and to correct the measured correlation time  $\tau_c$  for solvent viscosity and possible change of geometry or solvation. The dipole-dipole contribution  $T_1^{\text{DD}}$  to the relaxation time  $T_1$  and the correlation time of the molecule  $\tau_c$  are linked by the relation<sup>23</sup>

$$(T_1^{\text{DD}})^{-1} = \frac{1}{10} \left( \frac{\mu_0}{4\pi} \right)^2 \sum_i^n \left( \frac{\gamma_c \gamma_H \eta}{2\pi} \right)^2 \times \rho_{\text{CH}_i}^{-6} [J_0(\omega_H - \omega_C) + 3J_1\omega_C + 6J_2(\omega_H + \omega_C)] \quad (5)$$

(SI units;  $\gamma_c, \gamma_H$ : gyromagnetic ratios of  $^{13}\text{C}$  and  $^1\text{H}$  nuclei;  $\rho_{\text{CH}_i}$ : through-space  $^{13}\text{C}$ -proton  $i$  distance;  $\omega_H, \omega_C$ : Larmor pulsations of  $^1\text{H}$  and  $^{13}\text{C}$  nuclei;  $J_0, J_1, J_2$ : spectral density functions describing the frequency distribution of internuclear vector  $\rho_i$  movement).

Assuming isotropic molecular reorientation, the correlation time  $\tau_c$  corresponds to

$$J_0(\omega) = J_1(\omega) = J_2(\omega) = \frac{\tau_c}{1 + \omega^2 \tau_c^2} \quad (6)$$

Table 2 presents the  $^{13}\text{C}$ -NMR longitudinal relaxation times  $T_1$  measurements performed on a solution of the precursor **7** of CD-NA in  $\text{CD}_2\text{Cl}_2$  (30 mg/0.5 mL) at 294 K. The observed values for carbon atoms carrying at least one hydrogen atom are low and consistent with the values that have been observed for previous  $\beta$ -cyclodextrin derivatives.<sup>24</sup> As it was at that time underlined, the shortness of the longitudinal relaxation times  $T_1$  strongly suggests that the dipole-dipole interaction is the major component in the relaxation mechanism. Equation 6 was therefore used to calculate the correlation times  $\tau_c$  of the carbon atoms carrying at least one hydrogen atom. It arises from this calculation that the perester precursor **7** of CD-NA can be described as a poorly mobile core ( $\tau_c \approx 0.35$  ns) bearing more mobile naphthoyl chromophores ( $\tau_c \approx 0.22$  ns). This estimate of the correlation time is in agreement with the value predicted from application of the equation

$$\tau_c = \frac{4\pi a^3 \eta}{3kT} \quad (7)$$

where  $\eta$  and  $a$  are respectively the viscosity of the medium and the hydrodynamic molecular radius. If taking  $a = 1$  nm and  $\eta = 0.39 \times 10^{-3}$  Pa s,<sup>25</sup> the predicted correlation time  $\tau_c$  is equal to 0.4 ns, which is in line with the measurements. Equation 7 was then used to derive the correlation time of CD-NA. The correction of solvent viscosity provides  $\tau_c(\text{CD-NA}) = 0.7$  ns.

(23) Doddrell, D.; Glushko, V.; Allerhand, A. *J. Chem. Phys.* **1972**, *56*, 3683.

(24) Canceill, J.; Jullien, L.; Lacombe, L.; Lehn, J.-M. *Helv. Chim. Acta* **1992**, *75*, 791.

(25) Kinematic viscosity of methylene chloride at 303 K.



**Table 1.** Steady-State Emission Anisotropy<sup>a</sup> and Decay Time<sup>b</sup> of DCM-OH

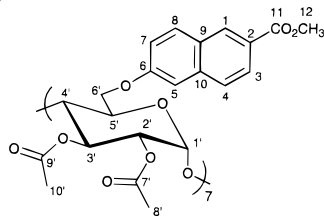
	$\bar{r}$	$\tau$ (ns)	$f^c$	$\chi_r^{2,d}$
glycerol at -5 °C	0.390			
pH 10 buffer at 25 °C without CD-NA	0.151	0.48 ± 0.07	1	1.85 <sup>e</sup>
pH 10 buffer at 25 °C with CD-NA (6.2 × 10 <sup>-5</sup> M) ([CD-NA]/[DCM-OH] = 18.8)	0.133	$\tau_1 = 2.52 \pm 0.03$ $\tau_2 = 0.55 \pm 0.07$	$f_1 = 0.940 \pm 0.003$ $f_2 = 0.06$	1.22 <sup>f</sup>
pH 10 buffer at 25 °C with CD-NA (1.2 × 10 <sup>-5</sup> M) ([DCM-OH]/[CD-NA] = 4)		$\tau_1 = 2.53 \pm 0.03$ $\tau_2 = 0.47 \pm 0.01$	$f_1 = 0.547 \pm 0.004$ $f_2 = 0.453$	1.95 <sup>f</sup>

<sup>a</sup> Measured on the SLM 8000C spectrofluorometer (excitation at 500 nm and observation at 600 nm). <sup>b</sup> Determined by multifrequency phase-modulation fluorometry (excitation at 442 nm and observation through a Schott GG495 cut-off filter:  $\lambda > 495$  nm). DCM in dimethyl sulfoxide was used as a reference ( $\tau = 2.33$  ns). <sup>c</sup> Fractional intensities. <sup>d</sup> Reduced chi-square. <sup>e</sup> Value obtained with standard deviations of 0.4° and 0.005 for phase shift and modulation ratio, respectively. <sup>f</sup> Value obtained with standard deviations of 0.2° and 0.004 for phase shift and modulation ratio, respectively.

**Table 2.** <sup>13</sup>C-NMR Longitudinal Relaxation Time  $T_1$  and Correlation Times  $\tau_c$  for the Carbon Atom Carrying at Least One Hydrogen Atom of the Precursor **7** of CD-NA in CD<sub>2</sub>Cl<sub>2</sub><sup>a</sup>

C atom	$\delta$ (ppm)	$T_1$ (s)	$\tau$ (ns)
7' or 9'	170.77	6.60	
7' or 9'	169.86	1.15	
11	166.95	5.65	
6	158.21	1.40	
10	136.87	3.55	
4	131.37	0.25	0.22
1	130.67	0.25	0.22
9	128.30	4.30	
3	126.89	0.25	0.22
8	126.25	0.25	0.19
2	119.24	0.25	0.22
7	107.27	0.25	0.21
1'	97.95	0.15	0.35
4'	77.41	0.15	0.35
3'	71.32	0.15	0.35
5'	71.16	0.15	0.38
2'	70.78	0.15	0.35
6'	67.70	0.095	0.27
12	52.24	0.45	
8' and 10'	21.08	0.60	

<sup>a</sup> Recording conditions: 30 mg of **7** in 0.5 mL of CD<sub>2</sub>Cl<sub>2</sub>, 4.7 T, 294 K. The correlation times were calculated using eq 5 with the assumption of isotropic rotational reorientation for atoms belonging to the CD core or to the naphthoyl ring when bearing one proton. Parameters used:  $n_H = 1$  (2 for  $\delta$  67.7 ppm),  $r_{CH} = 0.109$  nm,  $\omega_H(4.7 \text{ T})/2\pi = 200.00$  MHz,  $\omega_C(4.7 \text{ T})/2\pi = 50.288$  MHz;  $\hbar/2\pi = 1.0546 \times 10^{-34} \text{ m}^2\cdot\text{kg}\cdot\text{s}^{-1}$ ;  $\gamma_H = 2.675 \times 10^8 \text{ rad}\cdot\text{s}^{-1}\cdot\text{T}^{-1}$ ;  $\gamma_H = 3.977\gamma_C$ ;  $\mu_0 = 4\pi \cdot 10^{-7} \text{ m}\cdot\text{kg}\cdot\text{s}^{-2}\cdot\text{A}^{-2}$ .

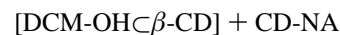


Taking into consideration (i) that  $a$  corresponds to the hydrodynamic molecular radius and that the solvation shell is probably thicker for CD-NA than for **7** in CD<sub>2</sub>Cl<sub>2</sub> due to the nature of the interactions involved in the solvation and (ii) that the DCM-OH correlation time is measured for a [DCM-OH⊂CD-NA] complex and so that the effective hydrodynamic radius of this complex may be larger than that of empty CD-NA, this estimate of the correlation time of CD-NA as estimated by <sup>13</sup>C-NMR spectroscopy compares well with the correlation time of complexed DCM-OH as measured by fluorescence spectroscopy. Moreover, it strongly suggests that the complex formed between CD-NA and DCM-OH is indeed tight, DCM-OH being rigidly held by CD-NA as long as DCM-OH rotational motions around the  $\beta$ -cyclodextrin symmetry axis are not considered.

**Table 3.** Thermodynamical Data for DCMOH Complexation by CD-NA or  $\beta$ -CD as Obtained from the Van't Hoff Analysis of the Complexation Constant  $K_{CD-NA}$  and  $K_{\beta-CD}$ 

	CD-NA	$\beta$ -CD
$\log K$	5.1	2.7
$\Delta_R G_{298}^\circ$ (kJ·mol <sup>-1</sup> )	-28.5 ± 0.8	-15.5 ± 1
$\Delta_R H_{298}^\circ$ (kJ·mol <sup>-1</sup> )	-8.6 ± 0.4	-4.7 ± 0.5
$\Delta_R S_{298}^\circ$ (J·K <sup>-1</sup> ·mol <sup>-1</sup> )	67 ± 3	36 ± 4

**Thermodynamics of Association.** The formation constant  $K_{CD-NA}^{298}$  of [DCM-OH⊂CD-NA] belongs to the largest ever measured for a  $\beta$ -cyclodextrin derivative.<sup>26</sup> In order to clear the origin of this large value, the complexation constant  $K_{\beta-CD}$  of DCM-OH in  $\beta$ -cyclodextrin ( $\beta$ -CD) was first measured by recording the fluorescence spectra of DCM-OH at constant DCM-OH concentration in the presence of increasing amounts of  $\beta$ -CD. Analysis of the data according to eq 3 by assuming a 1:1 complex stoichiometry provides a value of  $K_{\beta-CD}^{303}$  equal to  $500 \pm 15$  at 30 °C. This stability constant of [DCM-OH⊂ $\beta$ -CD] conforms to the value expected for the complexation of a benzene derivative, and the comparison with  $K_{CD-NA}^{298}$  emphasizes the contribution of the naphthoyl groups to increase the complex stability. To determine the thermodynamic parameters associated to the complexation reaction, the complexation constants  $K_{CD-NA}$  and  $K_{\beta-CD}$  were measured at different temperatures and analyzed according to the Van't Hoff relation by assuming constant values of standard reaction enthalpies  $\Delta_R H^\circ$  in the range of observed temperatures (Table 3). The observed values compare well with the linear energy relationship  $\Delta_R H^\circ$  vs  $-T\Delta_R S_{298}^\circ$  described in the literature<sup>26</sup> for host-guest complexation in the cyclodextrin series; in both CD-NA and  $\beta$ -CD cases, the complexation is mostly entropy-driven, the entropic term  $-T\Delta_R S_{298}^\circ$  representing about 70% of the free energy of complexation. The difference of complexation behavior of DCM-OH by CD-NA and  $\beta$ -CD can be explained on the basis of the reaction



with  $\Delta\Delta_R H_{298}^\circ = -3.9 \text{ kJ}\cdot\text{mol}^{-1}$  and  $\Delta\Delta_R S_{298}^\circ = 31 \text{ J}\cdot\text{K}^{-1}\cdot\text{mol}^{-1}$ . The DCM-OH interaction with the naphthoate residues provides an additional enthalpic contribution whereas the outer location of a large part of the DCM-OH molecule in [DCM-OH⊂ $\beta$ -CD] compared to [DCM-OH⊂CD-NA] and possibly a poorer lateral solvation of the naphthoyl chromophores in CD-NA compared to [DCM-OH⊂CD-NA] gives an additional large entropic contribution.

### Mechanism of Energy Transfer

We now turn our attention to the nature of the mechanisms of homotransfer (i.e., between naphthoate chromophores) and

(26) Inoue, Y.; Hakushi, T.; Liu, Y.; Tong, L. H.; Shen, B. J.; Jin, D. S. *J. Am. Chem. Soc.* **1993**, *115*, 475 and references therein.

heterotransfer (i.e., from naphthoate chromophores to DCM-OH included in the cavity) and to the competition between these two processes.

**Homotransfer.** In the preceding paper of this series,<sup>12</sup> we studied energy hopping in a multichromophoric cyclodextrin with seven naphthoyloxy chromophores attached to the secondary rim so that the average interchromophoric distance was about 8 Å. Time-resolved emission anisotropy in a rigid medium showed that the energy-hopping process was mainly governed by Förster's dipole-dipole mechanism.<sup>27</sup>

In CD-NA, the naphthoate chromophores are attached to the primary rim so that the distance between the links of the chromophores to the rim is about 4 Å. Keeping in mind in addition that the complex [DCM-OH⊂CD-NA] is tight (*vide supra*), special attention should be paid to short-range interactions resulting from interchromophore orbital overlap.

The relative contribution of Coulombic and short-range interactions is an important point to be discussed in light of the model recently proposed by Scoles and Ghiggino<sup>28</sup> for a pair of identical chromophores (e.g., naphthalene dimer). This model unifies excimer stability, molecular exciton interactions and interchromophore singlet-singlet electronic energy transfer. The authors showed that at both short range (ca. 3–6 Å) and intermediate range (ca. 6–20 Å), the electronic coupling can be written as

$$u = u^{\text{Coul}} + u^{\text{short}}$$

where  $u^{\text{Coul}}$  is the Coulombic interaction and  $u^{\text{short}}$  expresses the interactions that depend upon the degree of interchromophore orbital overlap.  $u^{\text{short}}$  is the sum of two terms: (i)  $u^{\text{exch}}$  defining the quantum mechanical two-electron-exchange interaction and (ii)  $u^{\text{pen}}$  accounting for interpenetration of the orbitals centered on the two chromophores. Therefore, interpenetration as well as exchange effects are important at close separations, whereas Dexter<sup>29</sup> discussed only the exchange interaction. Interestingly, the  $u^{\text{pen}}$  term acts to reinforce the  $u^{\text{Coul}}$  term, while  $u^{\text{exch}}$  opposes it. Regarding the Coulombic interaction, which is as usual described by a multipole expansion, Scholes and Ghiggino showed that in a pair of chromophores with dipole-allowed electronic transitions, the major contribution arises not only from dipole-dipole interactions but also from dipole-octopole and octopole-octopole interactions. About the relative contribution of the Coulombic and short-range interactions, these authors obtained very interesting results in the case of naphthalene dimers: for instance, at an interchromophoric distance as short as 4 Å, the contribution of short-range interactions to the overall calculated electronic coupling is only 17%.

Consequently, the major contribution to homotransfer between naphthoate chromophores in CD-NA, and its complex with DCM-OH, arises from Coulombic interaction despite the very short interchromophoric distances. This point will be further examined in a forthcoming paper describing emission anisotropy experiments performed with various  $\beta$ -cyclodextrins labeled with chromophores on the primary rim.

**Heterotransfer.** Since the complex [DCM-OH⊂CD-NA] is tight (*vide supra*), the distance between naphthoate residues and the distance between a naphthoate residue and a DCM-OH molecule within the cavity may be short enough to allow the molecular orbitals of the former to overlap those of latter. The above considerations on electronic coupling between two identical chromophores still apply in the case of two interacting nonidentical chromophores, and the conclusions are equally

valid.<sup>28</sup> Therefore, the Coulombic interaction is again likely to be predominant.

One now faces the question as to whether energy transfer occurs from naphthoate monomers to DCM-OH or from naphthoate excimers to DCM-OH or from both. If excimers still exist in the complex, the probability of transfer from them is higher than from the monomeric form since the spectral overlap is smaller in the latter case. However, it is likely that formation of the complex hinders excimer formation because, as mentioned above, the most probable conformation of excimers (in the absence of DCM-OH) is head to tail since the negative charges are kept away in such a conformation. However, we have no evidence of excimer hindrance on complexation because no fluorescence from the naphthoate groups of the complex could be detected.

Despite the fact that the validity of Förster's theory<sup>27</sup> is questionable at short distances where the point dipole approximation is not fulfilled, it is worth calculating the expected efficiency and rate constant for transfer from this theory in order to see whether these values are consistent with the experimental observations. With this aim, let us calculate the Förster critical radius rewritten as

$$R_0 = 0.2108[\kappa^2 \phi_D n^{-4} \int_0^\infty I_D(\lambda) \epsilon_A(\lambda) \lambda^4 d\lambda]^{1/6} \quad (8)$$

with  $R_0$  in Å, where  $\kappa^2$  is the orientational factor,  $\phi_D$  is the donor fluorescence quantum yield,  $n$  is the average refractive index of the medium in the wavelength range where spectral overlap is significant,  $I_D(\lambda)$  is the normalized fluorescence spectrum of the donor,  $\epsilon_A(\lambda)$  is the acceptor absorption coefficient (in  $\text{dm}^3 \cdot \text{mol}^{-1} \cdot \text{cm}^{-1}$ ), and  $\lambda$  is the wavelength in nanometers.

In a first approach, we assume that energy transfer occurs only from the monomer for the reason explained above. Then, for the calculation of the overlap integral, we must first extract the monomer band from the fluorescence spectrum of CD-NA. This can be achieved by using the fluorescence spectrum of the model compound Me-NA (Figure 2). Appropriate normalization and blue shift of this spectrum by 3 nm has been performed in order to obtain satisfactory superimposition with the blue edge of the CD-NA spectrum. It was then easy to decompose the overall fluorescence spectrum into the monomer and excimer bands and thus to determine the relative fluorescence quantum yields of these species (52.4% and 47.6% for the monomer and the excimer, respectively) and to calculate the overlap integral. The overall fluorescence quantum yield of CD-NA being 0.075 (see the Experimental Section), the fluorescence quantum yield of the monomer is then 0.039.

In similar labeled CD's investigated in one of our previous papers,<sup>10</sup> orientation of the naphthoyloxy residues was demonstrated to be essentially random, and fast local motions occur during the lifetime of the excited state. This led us to assume that the orientation factor was equal to the dynamic average, i.e.  $2/3$ . However, this assumption may not be valid in the present case since the complex was shown to be tight. Nevertheless, only an order of magnitude is searched for the efficiency and rate of transfer.

The index of refraction was chosen to be that of tetrahydrofuran (1.407) since this solvent mimicks the interior of the CD cavity. Under these conditions, the value of  $R_0$  calculated by means of eq 5 is  $23.5 \pm 1.5$  Å. The standard error takes into account the uncertainty on the fluorescence quantum yield (which might be higher in the absence of excimer formation) and on the index of refraction (if  $n = 1.3$  or  $1.5$  instead of  $1.4$ ,  $R_0$  is increased or decreased by 1 Å).

The value of the transfer efficiency can then be calculated by the usual expression

(27) Förster, Th. *Z. Naturforsch.* **1949**, 4a, 321.

(28) Scholes, G. D.; Ghiggino, K. P. *J. Phys. Chem.* **1994**, 98, 4580.

(29) Dexter, D. L. *J. Chem. Phys.* **1953**, 21, 836.

$$\Phi_T = \frac{1}{1 + (R/R_0)^6} \quad (9)$$

For instance, the transfer efficiency is expected to be 0.9999 at a donor–acceptor distance of 5 Å and 0.994 at 10 Å; these values are very close to 1, which agrees with the experimental value.

With regard to the rate constant for transfer, the expression for the Förster mechanism is

$$k_T^{d-d} = \frac{1}{\tau_D} \left( \frac{R_0}{R} \right)^6 \quad (10)$$

where  $\tau_D$  is the lifetime of the donor (in the absence of acceptor). For distances of 5–10 Å, the rates are  $1.8 \times 10^{12}$  to  $2.8 \times 10^{10} \text{ s}^{-1}$  for  $\tau_D = 5.95 \text{ ns}$  (this value was measured with Me-NA).

If we assume that some excimers are not broken upon binding of DCM-OH, the decomposition of the fluorescence spectrum allowed us to calculate the overlap integral which leads to  $R_0 = 27.5 \pm 1.5 \text{ Å}$ . The larger integral overlap explains that this value of  $R_0$  is greater than in the case where transfer would occur only from the monomer species. Consequently, if transfer can occur from excimer species, it is even more efficient and faster.

#### Competition between Homotransfer and Heterotransfer.

The question arises as to whether a naphthoate group that has just been excited by absorption of a photon transfers directly its excitation energy to an included DCM-OH molecule or whether energy hopping among the naphthoate groups has time to occur before transfer to DCM-OH. At the present stage of this study, it is not possible to answer this question; information on this point is in principle contained in the fluorescence decay of the donor groups (naphthoate) but, as shown above, it was not possible to observe such a decay because it was much too fast with respect to the time resolution of our apparatus. Nevertheless, it is worth noting that the emission spectrum of the naphthoate groups overlaps more strongly the absorption spectrum of DCM-OH than the absorption spectrum of these groups, so that energy transfer to DCM-OH is expected to be faster than homotransfer; this supposes of course that the average distance between a naphthoate group and a DCM-OH molecule is not significantly larger than the distance between naphthoate groups. Further studies using faster time-resolved spectroscopic techniques are required for a better understanding of the primary events of the excited-state processes.

#### Conclusion

The transfer of excitation energy from the naphthoyl chromophores of CD-NA toward a merocyanine, DCM-OH, included in the cavity takes place with an efficiency close to 1. The stability of the 1:1 complex is higher than expected from previously reported data on complexes with  $\beta$ -CD owing to the contribution of the naphthoate residues. Fluorescence polarization and  $^{13}\text{C}$ -NMR experiments provide evidence for tight complexes. In spite of the short distances between like or unlike chromophores in such complexes, it is likely that the Coulombic interaction has a much larger contribution in the mechanism of energy transfer than the short-range interactions.

Complexes of CD-NA with DCM-OH can be considered as supramolecular photochemical devices capable of efficient light conversion via the antenna effect and thus mimic important features of photosynthetic units. Another important aspect of multichromophoric cyclodextrins is their use as photochemical microreactors performing antenna-induced photoreactions within the cavity. Specific effects are to be expected from selective

excitation of the reactants included in the cavity by means of energy transfer from the appended chromophores. Investigations are in progress along this line. We have recently studied the case of unimolecular photoreactions exemplified with the photoisomerization of a nitron within CD-NA's cavity.<sup>30</sup>

#### Experimental Section

**General Procedures.** Anhydrous solvents (SDS), kept on molecular sieves (3–4 Å), were used as obtained. All catalytic hydrogenations were performed at 1 bar of pressure. Column chromatography (CC): silica gel 60 (0.040–0.063 mm) Merck. Analytical and preparative thin layer chromatography (TLC): silica gel plates Merck; detection by UV (254 nm),  $\text{I}_2$ , 5%  $\text{H}_2\text{SO}_4$  or  $[\text{MoO}_4(\text{NH}_4)_2]$  (2.5 g),  $(\text{NH}_4)_2\text{Ce}(\text{NO}_3)_6$  (1.2 g),  $\text{H}_2\text{SO}_4$  (100 mL, 3.6 M). Melting point: Kofler hot-stage.  $^1\text{H}$ -NMR spectra: AM-200-SY-Bruker (4.7 T); Aspect 3000 calculator; chemical shifts in parts per million related to protonated solvent as internal reference ( $^1\text{H}$ :  $\text{CHCl}_3$  in  $\text{CDCl}_3$ , 7.26 ppm;  $\text{CHD}_2\text{-SOCD}_3$  in  $\text{CD}_3\text{SOCD}_3$ , 2.49 ppm.  $^{13}\text{C}$ :  $^{13}\text{CDCl}_3$  in  $\text{CDCl}_3$ , 76.9 ppm,  $^{13}\text{CD}_3\text{SOCD}_3$  in  $\text{CD}_3\text{SOCD}_3$ , 39.6 ppm); coupling constants  $J$  in hertz. Mass spectrometry: FAB-MS (positive mode) was performed by the Service de Spectrométrie de masse du CNRS, Vernaion. Microanalyses were performed by the Service de Microanalyses de l'Université Pierre et Marie Curie, Paris. The per-2,3-diacetyl,per-6-iodo- $\beta$ -cyclodextrin was synthesized according to the literature.<sup>13</sup>

**6-(Benzyloxy)-2-bromonaphthalene (2).** A solution of 6-bromonaphth-2-ol (**1**) (10.0 g, 45 mmol) and benzyl bromide (12 mL, 49 mmol) in dry DMF (80 mL) was added dropwise into a suspension of NaH 60% (1.5 g, 45 mmol) in dry DMF (20 mL). The mixture was stirred at 70 °C for 22 h. After cooling, the solution was poured onto crushed ice. The resulting precipitate was filtered and thoroughly washed with water, then pentane. After drying, **2** was obtained as white crystals (10.6 g, 75%): mp 110 °C;  $^1\text{H}$ -NMR ( $\text{CDCl}_3$ ) 7.93 (s, 1H), 7.67 (d,  $J = 9 \text{ Hz}$ , 1H), 7.60 (d,  $J = 9 \text{ Hz}$ , 1H), 7.49 (d,  $J = 9 \text{ Hz}$ , 1H), 7.47–7.34 (m, 5H), 7.24 (d,  $J = 9 \text{ Hz}$ , 1H), 7.20 (s, 1H), 5.21 (s, 2H). Anal. Calcd for  $(\text{C}_{17}\text{H}_{13}\text{BrO})$  (313.2): C, 65.19; H, 4.18. Found: C, 65.17; H, 4.19.

**6-(Benzyloxy)-2-cyanonaphthalene (3).** A suspension of CuCN (5.43 g, 61 mmol) and **2** (9.50 g, 30 mmol) in dry DMF (100 mL) was stirred at 150 °C for 24 h. The mixture was extracted with ethyl acetate, the organic phase was extensively washed with NaCl brine and was then dried on  $\text{Na}_2\text{SO}_4$ . After evaporation of the solvent, the crude residue was purified by column chromatography (elution:  $\text{CH}_2\text{Cl}_2$ ) to provide **3** as a white powder (4.80 g, 61%): mp 138 °C;  $^1\text{H}$ -NMR ( $\text{CDCl}_3$ ) 8.14 (s, 1H), 7.81 (d,  $J = 8 \text{ Hz}$ , 1H), 7.77 (d,  $J = 7 \text{ Hz}$ , 1H), 7.57 (d,  $J = 7 \text{ Hz}$ , 1H), 7.51–7.39 (m, 5H), 7.33 (d,  $J = 7 \text{ Hz}$ , 1H), 7.23 (s, 1H), 5.21 (s, 2H). Anal. Calcd for  $(\text{C}_{18}\text{H}_{13}\text{NO})$  (259.3): C, 83.37; H, 5.05. Found: C, 83.25; H, 5.09.

**6-(Benzyloxy)-2-naphthoic Acid (4).** A mixture of **3** (3.90 g, 15 mmol) and NaOH 10 M (8.5 mL, 85 mmol) in ethylene glycol monomethyl ether (60 mL) was refluxed for 8 h. After cooling, the mixture was extracted with ethyl acetate. The aqueous phase was neutralized with HCl (0.1 M). The precipitate was filtered and extensively washed with water to give **4** as a white powder (2.80 g, 67%): mp 236 °C;  $^1\text{H}$ -NMR ( $\text{CDCl}_3/\text{DMSO}-d_6$ ) 8.54 (s, 1H), 8.01 (d,  $J = 8.5 \text{ Hz}$ , 1H), 7.94 (s, 1H), 7.85 (d,  $J = 8.5 \text{ Hz}$ , 1H), 7.55 (d,  $J = 8.5 \text{ Hz}$ , 1H), 7.48–7.29 (m, 6H), 7.34 (d,  $J = 7 \text{ Hz}$ , 1H), 5.27 (s, 2H). Anal. Calcd for  $(\text{C}_{18}\text{H}_{14}\text{O}_3)$  (278.3): C, 77.68; H, 5.07. Found: C, 77.55; H, 5.03.

**Methyl 6-(Benzyloxy)-2-naphthoate (5).** DCC (1.96 g, 9.5 mmol) was added portionwise at 0 °C into a solution of **4** (2.66 g, 9.5 mmol), DMAP (1.20 g, 9.5 mmol) in  $\text{CH}_2\text{Cl}_2$  (30 mL), and MeOH (2 mL, 38 mmol). After the solution was stirred at room temperature for 5 h, the suspension was filtered off. The filtrate was washed with HCl (1.2 M), then saturated  $\text{NaHCO}_3$  aqueous solution, and was dried on  $\text{Na}_2\text{SO}_4$ . After evaporation of the solvent, **5** was obtained as a white powder (2.25 g, 81%): mp 150 °C;  $^1\text{H}$ -NMR ( $\text{CDCl}_3$ ) 8.53 (s, 1H), 8.12 (d,  $J = 8.5 \text{ Hz}$ , 1H), 7.86 (d,  $J = 8.5 \text{ Hz}$ , 1H), 7.74 (d,  $J = 8.5 \text{ Hz}$ , 1H), 7.57–7.25 (m, 9H), 5.20 (s, 2H), 3.97 (s, 3H). Anal. Calcd for  $(\text{C}_{19}\text{H}_{16}\text{O}_3 \cdot 0.25\text{H}_2\text{O})$  (296.8): C, 76.90; H, 5.56. Found: C, 76.91; H, 5.46.

(30) Wang, P. W.; Jullien, L.; Valeur, B.; Filhol, J.-S.; Canceill, J.; Lehn, J.-M. *New J. Chem.*, in press.

**Methyl 6-Hydroxy-2-naphthoate (6).** A suspension of **5** (2.15 g, 7.4 mmol) and Pd/C 10% (500 mg) in  $\text{CH}_2\text{Cl}_2$  (50 mL) and MeOH (25 mL) was stirred under a hydrogen atmosphere at room temperature for 24 h. After filtration and evaporation of the solvent, the crude residue was recrystallized in chloroform to give **6** as a white powder (0.86 g, 57%): mp 170 °C;  $^1\text{H-NMR}$  ( $\text{CDCl}_3$ ) 10.2 (s, 1H), 8.48 (s, 1H), 7.96 (d,  $J = 8.5$  Hz, 1H), 7.75 (d,  $J = 8.5$  Hz, 1H), 7.18 (s, 1H), 7.15 (d,  $J = 8.5$  Hz, 1H), 3.86 (s, 3H); TLC (AcOEt)  $R_f = 0.3$ . Anal. Calcd for ( $\text{C}_{12}\text{H}_{10}\text{O}_3$ ) (202.2): C, 71.28; H, 4.99. Found: C, 71.16; H, 5.02.

**$2^{\text{A}}, 2^{\text{B}}, 2^{\text{C}}, 2^{\text{D}}, 2^{\text{E}}, 2^{\text{F}}, 2^{\text{G}}, 3^{\text{A}}, 3^{\text{B}}, 3^{\text{C}}, 3^{\text{D}}, 3^{\text{E}}, 3^{\text{F}}, 3^{\text{G}}$ -Tetradecaacetate  $6^{\text{A}}, 6^{\text{B}}, 6^{\text{C}}, 6^{\text{D}}, 6^{\text{E}}, 6^{\text{F}}, 6^{\text{G}}$ -Heptakis(6-oxyethyl 2-naphthoate ester)  $\beta$ -Cyclodextrin **7**.** **6** (212 mg, 1.05 mmol, 3 equiv) was added under argon into a suspension of NaH 80% (30 mg, 1.05 mmol, 3 equiv) in dry DMF (3.5 mL; filtered on activated molecular sieves just before use and flushed with argon). After the mixture was stirred for 30 min at 70 °C and then cooled to room temperature under constant bubbling of argon, per-2,3-acetate, per-6-iodo  $\beta$ -cyclodextrin (125 mg, 0.05 mmol) was added and the mixture was further stirred under argon at room temperature for 2 h. After addition of water, the solution was extracted with ethyl acetate. The organic phase was extensively washed with water and dried over  $\text{Na}_2\text{SO}_4$ . The crude residue (215 mg) was purified by preparative TLC (first elution AcOEt–hexane (1:1); second elution  $\text{CH}_2\text{Cl}_2$ –MeOH (19:1) to give 107 mg of a white powder which was triturated with MeOH (0.5–1 mL) to give **7** as a white powder after filtration and washing by MeOH (95 mg, 63%):  $^1\text{H-NMR}$  ( $\text{CDCl}_3$ ) 8.17 (s, 1H), 7.58 (dd,  $J = 8.6$  Hz and  $J = 1.3$  Hz, 1H), 7.34 (d,  $J = 9.0$  Hz, 1H), 6.97–6.89 (m, 2H), 6.64 (s, 1H), 5.42 (t,  $J = 8.8$  Hz, 1H,  $\text{H}_3$ ), 5.16 (d,  $J = 3.8$  Hz, 1H,  $\text{H}_1$ ), 4.89 (dd,  $J = 3.8$  Hz and  $J = 9.3$  Hz, 1H,  $\text{H}_2$ ), 4.55–4.35 (m, 2H), 4.17 (d,  $J = 9.5$  Hz, 1H), 4.1–3.9 (m, 1H), 3.93 (s, 3H), 2.17 (s, 3H), 2.10 (s, 3H);  $^{13}\text{C-NMR}$  ( $\text{CDCl}_3$ ) 170.3, 169.3, 166.6, 157.7, 136.4, 131.0, 130.4, 127.9, 126.4, 126.0, 125.8, 118.7, 106.9, 97.4, 77.1, 71.0, 70.6, 70.1, 67.3, 51.9, 20.6. Anal. Calcd for ( $\text{C}_{22}\text{H}_{22}\text{O}_9$ ) (3012.8): C, 61.39; H, 5.15. Found: C, 60.86; H, 5.31. MS(FAB $^+$ ): chemical mass found 3012.3 (theoretical 3012). TLC: elution benzene–acetate (3:2)  $R_f = 0.45$ ; elution  $\text{CH}_2\text{Cl}_2$ –MeOH (19:1)  $R_f = 0.56$ .

**$6^{\text{A}}, 6^{\text{B}}, 6^{\text{C}}, 6^{\text{D}}, 6^{\text{E}}, 6^{\text{F}}, 6^{\text{G}}$ -Heptakis(6-oxy-2-naphthoic acid)  $\beta$ -Cyclodextrin **8**.**<sup>31</sup> A solution of tetramethylammonium hydroxide pentahydrate (85 mg, 0.047 mmol, 1.1 equiv) in water (2 mL) was added to a solution of **7** (60 mg, 0.02 mmol) in THF (3 mL) and the mixture was stirred at 60 °C for 24 h. After cooling, water was added ( $\approx 3$  mL) and the neutral parts were extracted with EtOAc. The aqueous phase was filtered on paper and then evaporated to dryness. The residue was triturated with acetic acid ( $\approx 1$ –2 mL). The obtained resin was filtered on a Büchner funnel and thoroughly washed with water to give **8** as a whitish powder (30 mg, 65%):  $^1\text{H-NMR}$  ( $\text{DMSO}-d_6$ ) 8.44 (s, 1H), 7.67 (d,  $J = 8.8$  Hz, 1H), 7.31 (d,  $J = 8.2$  Hz, 1H), 6.88 (d,  $J = 8.6$  Hz, 1H), 6.79 (s, 1H), 6.70 (d,  $J = 8.6$  Hz, 1H), 5.8 (bs, 1H), 4.91 (s, 1H), 4.21–4.15 (m, 3H), 3.76–3.08 (m, 3H).

**4-(Dicyanomethylene)-2-methyl-6-(*p*-(bis(hydroxyethyl)amino)-styryl)-4H-pyran (DCM-OH).** This compound was synthesized by Dr. J. Bourson according to the general procedure described in ref 32.

(31) The conditions of saponification were taken from the following reference: Chang, S. K.; Cho, I. *J. Chem. Soc., Perkin Trans. 1* **1986**, 211.

**Solvent.** The Britton–Robinson buffer at pH 10 (ionic strength of 0.1 M) was prepared according to ref 33.

**Spectroscopic Measurements.** The UV–vis absorption spectra were recorded on a Kontron Uvikon-940 spectrophotometer. Corrected fluorescence spectra and excitation polarization spectra were obtained with a SLM 8000 C spectrofluorometer. Steady-state fluorescence anisotropies defined as  $r = (I_{\parallel} - I_{\perp}) / (I_{\parallel} + 2 I_{\perp})$ , (where  $I_{\parallel}$  and  $I_{\perp}$  are the fluorescence intensities observed with vertically polarized excitation light and vertically and horizontally polarized emissions, respectively) were determined by the  $G$ -factor method.<sup>34</sup>

The overall fluorescence quantum yield of CD-NA was measured using 5-hydroxyquinoline in DMSO as a reference ( $\Phi_F = 0.19$ )<sup>35</sup> and found to be 0.075 (the refractive index of the pH 10 buffer containing 5% (v/v) of ethanol is 1.336).

The fluorescence quantum yield of DCM-OH in the buffer at pH 10 was determined by comparison with its known fluorescence quantum yield in DMSO (0.50)<sup>36</sup> and was found to be 0.073. In the presence of 18.8-fold excess of CD-NA, the fluorescence quantum yield is 0.36. This value does not represent the true quantum yield of DCM-OH in the CD-NA cavity because this solution contains a small amount of free DCM-OH. Then, correction using the fractional intensities provided by the time-resolved experiments (Table 1) leads to 0.38.

Time-resolved fluorescence experiments were carried out in both frequency and time domains. In frequency domain, we used our multifrequency (0.1–200 MHz) phase-modulation fluorometer described elsewhere.<sup>37</sup> The samples were excited at 442 nm with an Omnichrome He–Cd laser. The number of frequencies used was typically 20 for double-exponential decays.

In time domain, the single-photon timing technique<sup>38</sup> was used with picosecond laser excitation with a Spectra-Physics setup composed of a Titanium Saphir Tsunami laser pumped by an argon ion laser, a pulse selector, and doubling (LBO) and tripling (BBO) crystals. Pulses are 1 ps long. Light pulses are selected by an optoacoustic crystal at a repetition rate of 4 MHz. Fluorescence photons are detected with a Hamamatsu MCP photomultiplier R3809U. The constant fraction discriminator (Institute of Nuclear Physics in Orsay) is optimized for the output of MCP to which it is directly connected. The time-to-amplitude converter was purchased from Tennelec. With this setup, a minimum of 37 ps fwhm instrument response is achieved.

Both phase-modulation and time-correlated data were analyzed by a nonlinear least-squares method using Globals software (Globals Unlimited, University of Illinois at Urbana-Champaign, Laboratory for Fluorescence Dynamics).

JA954332T

(32) Bourson, J.; Valeur, B. *J. Phys. Chem.* **1989**, 93, 3871.

(33) Frugoni, C. *Gazz. Chim. Ital.* **1957**, 87, 403.

(34) Chen, R. F.; Bowman, R. L. *Science* **1965**, 147, 729.

(35) Goldman, M.; Wehry, E. L. *Anal. Chem.* **1970**, 42, 1178.

(36) Armand, X.; Bourson, J. Unpublished results.

(37) Pouget, J.; Mugnier, J.; Valeur, B. *J. Phys. E: Sci. Instrum.* **1989**, 22, 855.

(38) O'Connor, D. V.; Phillips, D. *Time-Correlated Single Photon Counting*; Academic: London, 1984; p 52.